The differential cross sections for inelastically scattered protons to the first 2^+ and 3^- states were found to be adequately explained by a distorted-wave calculation, assuming a collective vibrational model including complex coupling and Coulomb excitation. The large decreasing trends with increasing A observed in the inelastic cross sections are primarily accounted for by a decreasing collectivity. The deformation parameters deduced from these calculations are generally in agreement with those obtained from Coulomb excitation and other types of studies. Some differences arise, however, and further work in this area is desirable.

Note added in manuscript.

(1) Recent accurate results ($\pm 2\%$ relative errors) for $B(E2)$ values from Coulomb excitation of the even tin isotopes indicate a larger range of collectivity between ^{112}Sn and ^{124}Sn than shown by previous measurements [P. H. Stelson, F. K. McGowan, R. L. Robinson, W. T. Milner, and R. O. Sayer, Phys. Rev. **170**, 1172 (1968)]. This supports our conclusion that the differences in the 2^+ integrated cross sections for ^{112}Sn and ^{124}Sn are accounted for by a collectivity difference. Assuming a realistic rounded charge distribution with $r_0=1.07$ fm and $a=0.55$ fm [L. W. Owen and G. R. Satchler, Nucl. Phys. **51**, 155 (1964)] increases the Coulomb excitation β_2's by approximately 10%, so that the proton scattering and Coulomb excitation results agree on the average within 3%.

(2) Further optical-model analysis of the proton data, searching on the real central potential parameters V, r_0, and a, indicates that the volume integral of the real part of the potential divided by A and plotted against $(N-Z)/A$ (see Ref. 39) is consistent with a zero or small positive slope.

(3) A similar plot, obtained by searching on the six parameters in the real and imaginary parts of the optical potential, shows no definite slope. When the same analysis is applied to the imaginary part of the potential, the imaginary volume integral divided by A and plotted against $(N-Z)/A$ exhibits a positive slope in both cases.

ACKNOWLEDGMENTS

We wish to thank P. D. Kunz for providing us with the distorted-wave program DWUCK and helpful comments on its use. We are grateful for useful conversations with G. W. Greenlees and T. Tamura.

PHYSICAL REVIEW VOLUME 174, NUMBER 4 20 OCTOBER 1968

Levels in Even-Even Hg^{192}, Hg^{194}, Hg^{196}, and Hg^{198}†

R. F. PETRY,* R. A. NAUMANN,‡ AND J. S. EVANS§
Palmer Physical Laboratory, Frick Chemical Laboratory, and Princeton-Pennsylvania Accelerator, Princeton University, Princeton, New Jersey 08540

(Received 28 March 1968)

The decay of the 2^- and 7^+ isomeric states of Tl^{192}, Tl^{194}, Tl^{196}, and Tl^{198} has been studied, using isotopically separated sources produced by high-energy proton spallation of lead and uranium targets. γ-ray and conversion-electron spectra have been recorded, and extensive coincidence measurements have helped to establish the energy levels that are populated in the corresponding mercury daughter nuclides. Level schemes for Hg^{192}, Hg^{194}, Hg^{196}, and Hg^{198} deduced from the data are presented and discussed.

I. INTRODUCTION

THE modes of decay for both the high- and low-spin isomers of $Tl^{192,194,196,198}$ have been investigated in order to study the energy levels in the even-even daughter nuclei $Hg^{192,194,196,198}$. The thallium nuclides lie to the neutron-deficient side of the valley of β stability and can be reached only by high-energy proton-spallation reactions or by heavy-ion reactions. The desirability of studying nuclides lying away from the β-stability region has been discussed in recent articles by Bés[1] and by Bergström.[2] In addition, Bergström[3] has reviewed the experimental techniques available for such studies, especially the application of isotope separators.

The present work is part of a program to study neutron-deficient spallation products obtained from the bombardment of heavy targets with 3-GeV protons from the Princeton-Pennsylvania Accelerator (PPA). When a target of mass number A is irradiated with 3-GeV protons, the spallation products may have mass numbers from 1 to $A+1$. The Princeton electromagnetic isotope separator has been utilized to pick out of this complex mixture the particular isotope of interest. Isotopically pure samples with sufficient intensity for β-

† Work supported by the U. S. Atomic Energy Commission.
* Present address: Department of Physics, University of Oklahoma, Norman, Okla.
‡ Presently on leave at the Niels Bohr Institute, Copenhagen, Denmark.
§ Present address: Department of Chemistry, Lawrence University, Appleton, Wisc.

[1] D. R. Bés, Nucl. Instr. Methods **38**, 277 (1965).
[2] I. Bergström, Nucl. Instr. Methods **43**, 116 (1966).
[3] I. Bergström, Nucl. Instr. Methods **43**, 129 (1966).

and γ-ray spectroscopy have been obtained for a number of elements in the medium-to-heavy mass region. A description of the general technique has been published elsewhere.[4]

The separation and study of isotopes of thallium and mercury (and the gold and platinum decay products) were chosen to initiate the nuclear spectroscopy program at the PPA for three reasons: (1) These elements are easily separated from the target material by volatilization in the ion source of the isotope separator without need for prior chemical separation; (2) considerable interest is evinced in the nuclear levels of the isotopes of mercury and platinum because they lie in the transition region between the deformed rare-earth nuclei and the spherical nuclei in the region of doubly magic Pb^{208}; (3) some initial work had been done on these elements by workers at the Gustaf-Werner Institute[5] and at the Orsay Laboratory[6] that could serve as a guide for the present experiments. Previous information on the levels of even-even mercury isotopes with a mass less than 200 has been drawn from limited studies of the ground-state decay of Au^{196}, Au^{198}, and Tl^{198},[7] and the $(p,2n)$ reaction work of Sakai, Yamazaki, and Ejiri.[8] These studies were, by necessity, limited to the low-spin states that could be reached by β-decay processes from a spin-2 ground state or, in the case of the $(p,2n)$ work, by the low bombarding energies available. [Recent (as yet unpublished) $(p,2n)$ and $(p,4n)$ studies at higher bombarding energies have been made by Yamazaki and Hendrie in which they populate spin-6 and spin-7 states (see Ref. 9).] The electron-capture decay of high-spin isomers in thallium isotopes represents one way of reaching higher-spin states in the mercury daughters, and such isomers with a spin-parity of 7+ have been found by Jung and Andersson[10] and Andersson, Häller, and Ringh[11] for the isotopes Tl^{192}, Tl^{194}, Tl^{196}, and Tl^{198}. These authors measured the half-lives and the branching ratios between electron-capture and isomeric decay. Where possible, they reported other energy levels in each nucleus as revealed through the isomeric decay connecting the high- and low-spin states. Isomeric decay was especially pronounced only in Tl^{198} where 55% of the decay goes via an $M4$ transition to a lower-lying 3^- level. They also observed two strong $E2$ transitions, one at an energy of about 420 keV and a second at energies between 40 and 100 keV, that are converted in mercury and that follow the electron-capture decay of each of the 7^+ isomers.

The purpose of the experiments reported here was to extend the earlier study of these isomers with the expectation that high-spin levels in the mercury daughters would be populated. There have been two brief reports of this work giving preliminary data.[12,13] In the following section, preparation of sources and measurement techniques will be reviewed and some previously unreported innovations in source preparation will be described. The results of the measurements are presented in Sec. III, and construction of level schemes is covered in Sec. IV. In the final section, these level schemes will be compared with the results of other groups, available theoretical calculations, and nuclear level systematics.

II. EXPERIMENTAL TECHNIQUES

Preparation of Sources

Targets of either lead foil (0.25 mm) or uranium foil (0.125 mm) were irradiated for periods of 10–60 min in the PPA. In order to obtain a maximum target thickness for high yield while using as little target material as possible for ease of separation, the target was placed so that as the proton beam spiraled inward at the end of the acceleration cycle it intercepted the foil edgewise and traversed the plane of the foil. This technique can yield an effective target thickness of about 3.5 cm while the activity is contained in a strip of dimensions 3.5 by 0.6 cm.

After bombardment the target was removed to the isotope-separator laboratory and placed in the ion source of the isotope separator. The lead or uranium was heated to drive off the more volatile products including mercury and thallium. These atoms were ionized, accelerated to 60 keV, magnetically dispersed, and collected onto strips of aluminum foil at the collector end of the isotope separator. If time permitted, a radio-autograph was made of the collector foil to ensure that the focused mass lines matched previously inscribed fiducial marks. A sample radio-autograph is reproduced in Fig. 1. However, the placement of the lines was generally quite precise, and this latter step was often omitted for 10-min Tl^{192} in the interest of saving time. Once the foil was removed from the collector box of the separator it was cut into narrow strips which form suitable sources for γ-ray or conversion-electron measurements, including those made with an orange-type magnetic spectrometer. Separations were usually (but not always) quite clean, and cross contamination from adjacent masses was typically less than 1%. The elapsed time between the end of bombardment and the completion of the separation was routinely 15–20 min; with

[4] R. A. Naumann and G. Sidenius, Nucl. Instr. Methods **38**, 319 (1965).
[5] G. Andersson, Arkiv Fysik **12**, 331 (1957).
[6] N. Poffé, G. Albouy, R. Bernas, M. Gusakow, M. Riou, and J. Teilla, J. Phys. Radium **21**, 343 (1960).
[7] C. M. Lederer, J. M. Hollander, and I. Perlman, *Table of Isotopes* (John Wiley & Sons, Inc., New York, 1967), 6th ed.
[8] M. Sakai, T. Yamazaki, and H. Ejiri, Nucl. Phys. **74**, 81 (1965).
[9] T. Yamazaki and D. L. Hendrie, University of California Radiation Laboratory Report No. UCRL-17299 (unpublished).
[10] B. Jung and G. Andersson, Nucl. Phys. **15**, 108 (1960).
[11] G. Andersson, I. B. Häller, and R. Ringh, J. Inorg. Nucl. Chem. **17**, 15 (1961).
[12] R. F. Petry, R. A. Naumann, and J. S. Evans, Phys. Letters **21**, 541 (1966).
[13] R. A. Naumann, R. F. Petry, and J. S. Evans, Arkiv Fysik **36**, 177 (1967).

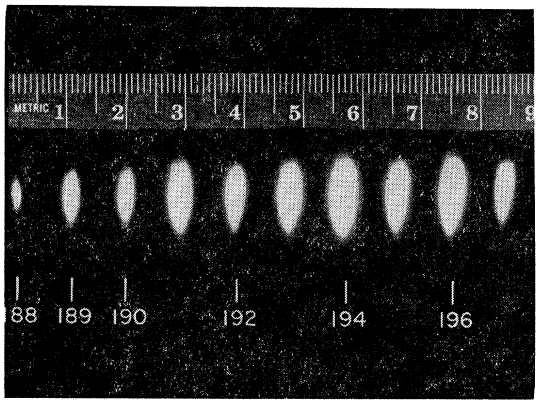

FIG. 1. Radio-autograph of the collector foil after a separation of isotopes from an irradiated lead target.

special effort this could be reduced to a minimum of 10 min.

Most of the sources used in these measurements were obtained by the method of collection just described. There were two occasions, however, when special collection techniques were employed. The first such technique was used to provide sources of Tl^{194}, Tl^{196}, and Tl^{198} for permanent-magnet spectrographs. These instruments require that the source be deposited on a thin wire, and a method had to be developed for collecting the ion beam on such wires. A potential difference of 30 keV was applied between a thin wire (0.4 mm diam) and a coaxial conductor to produce a cylindrically symmetric electric field. The ion beam initially moving perpendicularly to this field was converged toward the central wire by this field. This method proved quite successful, with as much as 90% of the separated activity collected on the wire in some trials.

The second special collection technique was devised in order to obtain sources of 10-min Tl^{192} relatively free of 4.9-h Hg^{192}. The latter occurs in separated mass-192 sources both as a daughter activity and as a primary spallation product. To minimize this contamination, special 10-min bombardments were followed by a two-stage separation procedure equivalent to a fractional distillation that exploits the difference in volatility of mercury and thallium. The temperature of the target was raised until radioactive mercury was detected at the collector box of the separator. The temperature was held at this level, with the collector foil covered, until the mercury was depleted (about 5 min). The collector foil was then uncovered and the temperature raised for the collection of thallium. Such a procedure yielded sources of Tl^{192} that were remarkably free of the longer-lived Hg^{192} as will be discussed in the next section.

Spectroscopic Measurements

γ-ray measurements were made with both NaI and Ge(Li) spectrometers. The NaI detectors were used primarily for initial survey and coincidence work. Detailed γ spectroscopy was performed with three Ge(Li) detectors during the course of the experiments. One, of the planar type, was fabricated in this laboratory and had an area of 4 cm^2 and a depletion depth of 6–7 mm. The other two detectors were of the coaxial type and were commercially produced. One of these had an active volume of 8 cm^3 and a depletion depth of 5 mm (Princeton Gamma-Tech); the other had an active volume of 8 cm^3 and a depletion depth of 11 mm (Nuclear Diodes). Each of these detectors, when in use, was coupled to a Tennelec TC130-TC200 preamplifier-amplifier system and a Nuclear Data ND-161 4096-channel analyzer. The system resolutions for these spectrometers for the 1.33-MeV line from Co^{60} were 4.0, 5.9, and 3.0 keV, respectively.

Most of the conversion-electron measurements were made with two Si(Li) detectors (TMC). These were operated at $-80°C$ to reduce leakage noise and were coupled to TC130-TC200 amplifier systems; the system resolutions for the two detectors were 6 and 3.7 keV for 400-keV electrons. In addition to the solid-state detectors, a permanent-magnet spectrograph was used to examine the very-low-energy part of the electron spectrum where Si(Li) spectra suffer from the steeply rising x-ray and Compton-electron background. The electron spectra were also scanned with an orange-type magnetic spectrometer, but the short half-lives involved in these experiments made precision measurements with this instrument difficult.

Both γ-γ and conversion-electron-γ coincidences were measured. For γ-γ coincidences, a NaI detector was used to provide a gate for either another NaI detector or a Ge(Li) detector, and two NaI detectors were used in a two-parameter mode. For triple coincidence work, three NaI detectors were used. Conversion-electron gates free of the Compton background encountered with NaI or Ge(Li) were provided by the orange spectrometer. In each coincidence experiment that involved a NaI gate, a coincidence spectrum was also accumulated with the gate just below the peak of interest in order to gauge the effect on the primary coincidence spectrum caused by real coincidences with the Compton background in the gate.

The γ-ray energies and relative intensities presented in the following section have been derived from Ge(Li) spectra calibrated with a set of standard sources. The standard spectra were taken either directly before or after the run with the sample, and care was taken to keep counting rates of the sample and the standard comparable in order to avoid gain shifts induced by marked changes in source intensity. In some instances a digital stabilizer was employed to ensure a constant gain while changing from sample to standard. The position of a 511-keV annihilation line that appears in each of the isotopes studied was used as an internal check on the calibration. The peak positions of both standard and unknown lines were determined by a computer program,

and the positions of the standard lines were least-squares fitted to a quadratic function of channel number. This method of energy determination works quite well over the central portion of the spectrum but larger deviations from the quadratic fit occur at the extremes, especially the low end, and larger uncertainties must be assigned to the energies of lines in these regions. The program is also used to subtract a linear background from each peak and to integrate the net peak area for use in determining relative γ-ray intensities.

The efficiencies of the Ge(Li) detectors had to be determined as a function of energy in order to obtain relative γ-ray intensities. A set of calibration sources whose disintegration rates were known to an accuracy of 2.3% was purchased from the International Atomic Energy Agency. A number of measurements employing these sources were made for each detector with various source-to-detector distances in order to average over any variations in geometry. With this method it was felt that efficiencies in the energy range 60–2000 keV were known to $\pm 20\%$ and in the more restricted range between 400 and 1500 keV to $\pm 10\%$.

The errors assigned to the γ-ray energies are obtained using rms deviations from the average of several determinations for each energy and from a consideration of possible systematic errors indicated by the inadequacy of a quadratic fit to the calibration points. Errors assigned to γ-ray intensities mainly result from counting statistics and from uncertainties in the efficiency calibrations of the Ge(Li) detectors.

The prior knowledge of the $E2$ character of the strong transition of approximately 420 keV observed in each even-even mercury isotope makes it possible to determine conversion coefficients for other lines by comparison of γ-ray and conversion-electron intensities with similar intensities for the 420-keV transitions. The conversion coefficient for the ith shell or subshell is given by

$$\alpha_i(E)=\frac{N_i(E)}{N_K(420)}\frac{N_\gamma(420)}{N_\gamma(E)}\alpha_K(420),$$

where $N(E)$ represents the integrated counts under either a γ-ray or conversion-electron line (as indicated) at transition energy E.

III. RESULTS

The similarity of the γ-ray spectra from each of these isotopes is striking. The spectrum following the decay of the high-spin isomers is dominated by four transitions, three of which lie in the energy range 400–800 keV and include the 420-keV $E2$ lines reported by Jung and Andersson[10] and by Andersson *et al.*[11] The fourth strong transition is the lower-energy $E2$ transition that these authors observed to follow the decay of each of the high-spin thallium isomers. We have located and measured the energy of these low-energy transitions and obtain good agreement with the energies reported except in the case of Tl^{192m} where we find an energy of 133.1 keV instead of the 109-keV $E2$ line listed in Ref. 11. From measurements with a permanent-magnet spectrograph we confirm that these transitions in Hg^{194}, Hg^{196}, and Hg^{198} are converted in mercury. Furthermore, all four of the dominant transitions are found to be in coincidence with each other. A number of weaker lines are also seen, and these form a more-or-less similar pattern from isotope to isotope.

Most of the sources for the study of these isomers were obtained from the spallation of lead targets. No appreciable change with time in the pattern of γ-ray intensities from these sources was observed with the exception of the mass-198 isotope. This is in agreement with the reported absence of any significant amount of isomeric decay for Tl^{192m}, Tl^{194m}, and Tl^{196m} and the very nearly equal half-lives for the decay of the high-spin and low-spin isomers in the mass-194 and -196 isotopes. Since the strongest transitions observed are known to follow the decay of the high-spin isomer, it is clear that thallium is separated as a primary spallation product and furthermore that the high-spin isomeric state is favored in the spallation reaction. In fact, we find from observing the growth of the ground-state decay in mass 198 that the ground-state yield is less than 10% of the yield for the high-spin isomer.

In order to assign transitions to a group following the decay of the 7^+ level or a group following the decay of the 2^- ground state, sources of the same isotopes were produced by the spallation of uranium targets. In this method of production it might be expected that the ground-state yield will be enhanced through electron-capture decay of higher-Z spallation products. This was, in fact, observed to be the case; transitions known to follow the decay of Tl^{198g} were enhanced by the feeding of the ground state from the decay of Pb^{198} separated from the uranium targets along with thallium and mercury. A similar change in the relative γ-ray intensities was observed for the mass-194 and -196 isotopes as well.

One further general comment is in order before presenting results for each isotope individually. The spectrum associated with the decay of each of the high-spin isomers is relatively simple and contains only a few lines below 1.5 MeV; none were detected above this energy. Such is not the case, however, for the ground-state decay. The proliferation of observed lines increased markedly when the ground-state decay was enhanced through use of uranium as a target, and in the decay of both Tl^{196} and Tl^{198} more than 100 transitions have been found in the energy range between 0.2 and 4.0 MeV. This complexity falls off as one proceeds to the lighter thallium isotopes, but this is probably only a consequence of the shorter half-lives and the more limited observation times. No attempt will be made in this publication to analyze all of these results. Efforts will be concentrated on those transitions following the

decay of the high-spin isomer and on a few of the stronger and more interesting transitions following the ground-state decay. However, energies and relative intensities of those transitions that can be reasonably identified with the decay of thallium are listed in the tables.

Tl^{192}

Because of the 11-min half-life and the growing contamination from the decay of Hg^{192} this isotope was the most difficult of the four to study. Two half-life determinations were made that yielded a mean value of 10.5 ± 1 min in agreement with Ref. 11.

Sample γ-ray spectra are shown in Fig. 2. Spectrum 2(A) was taken with a source separated from a lead target. The lines found to follow the decay of thallium are labeled; the other lines are associated with the decay of the Hg^{192} daughter, the Au^{192} granddaughter, and possible contaminants. Figure 2(B) contains a spectrum also taken from a source separated from lead, but after the fractional distillation technique had been developed. The improvement is obvious, especially in the low-energy region. A spectrum taken with a source separated from a uranium target is shown for comparison in Fig. 2(C) (no fractional distillation). Although the change is not nearly as marked as for the other isotopes, the relative intensities of the 674.2-, 691.0-, and 1113.0-keV transitions are enhanced compared with the same lines in Figs. 2(A) and 2(B).

Both NaI-Ge(Li) and two-parameter NaI-NaI γ-γ coincidence measurements were carried out, the former with the NaI detector used to gate on the 423.0-keV transition. The NaI-Ge(Li) coincidence results are shown in Fig. 2(D). The 423.0-keV peak appears in the spectrum because of the Compton events from the higher-energy transitions contained in the NaI gate. This was checked by setting the gate position just below the 423.0-keV peak. The excessive width of the higher-energy lines is apparently due to some instrumental effect (probably a gain shift) and also appears in similar coincidence spectra for Tl^{194}. From this spectrum and from the NaI-NaI two-parameter results, it is clear that the 423.0-keV transition is in coincidence with transitions at 133.1, 174.3, 634.7, 691.0, 745.3, and 786.1 keV. Also from the two-parameter results, it was established that the 133.1-, 423.0-, and 634.7-keV transitions are in mutual coincidence, and that a coincidence relation exists between the transitions at 174.3 and 745.3 keV.

Two conversion-electron spectra from a Si(Li) detector that were taken consecutively for 20 min each are

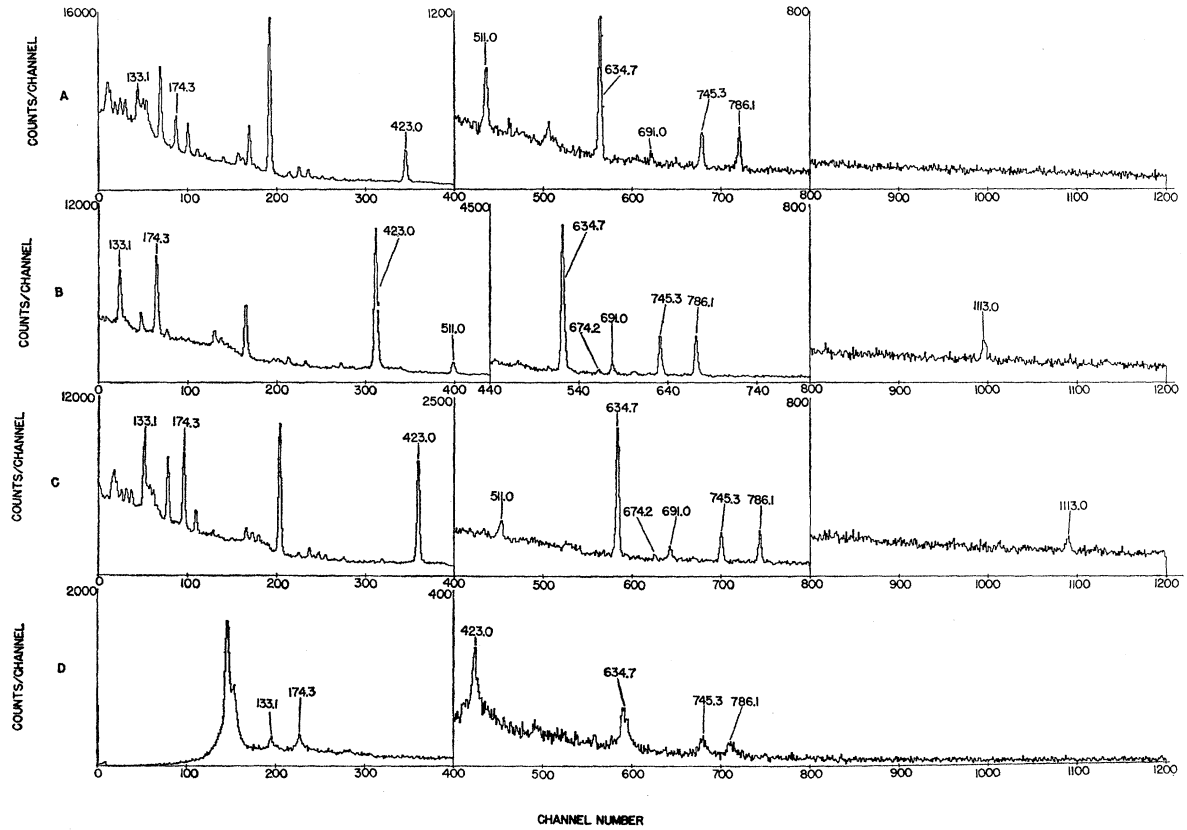

FIG. 2. γ-ray spectra from the decay of Tl^{192}: (A) from lead target, (B) from lead target with fractional distillation, (C) from uranium target, (D) in coincidence with the 423.0-keV line.

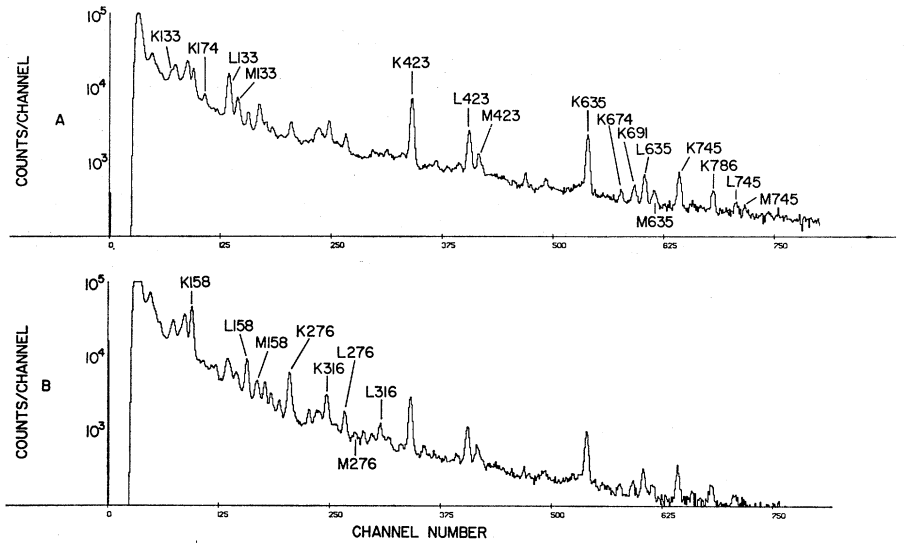

FIG. 3. Consecutive 20-min conversion-electron spectra from the decay of Tl^{192}.

shown in Fig. 3. In Fig. 3(A) the prominent lines associated with the decay of Tl^{192} are labeled while in Fig. 3(B) the labeled lines represent major transitions accompanying the decay of the Hg^{192} daughter. These spectra were taken from sources separated from lead with fractional distillation. Because of the similarity between the decay properties of Tl^{192} and the heavier even-mass thallium isotopes, it is nearly certain that both a spin-7 and a spin-2 isomer of Tl^{192} exist, each with an approximately 11-min half-life.

γ-ray energies and intensities for all four isotopes are listed in Table I. Conversion coefficients calculated from comparison of electron intensities with the intensities of the 420-keV lines (previously determined to be $E2$) are given in Table II along with theoretical values for comparison. Coincidence results for the four isotopes are summarized in Table III.

Tl^{194}

Half-life determinations for the decay of Tl^{194} yielded a value of 35.1 ± 1 min, slightly above the previously published value.[10] γ-ray spectra obtained from separated sources of Tl^{194} are shown in Fig. 4. Spectrum 4(A) was taken with a lead-separated source and a comparison can be made with a spectrum from a uranium-separated source in Fig. 4(B). Enhancement in Fig. 4(B) of lines

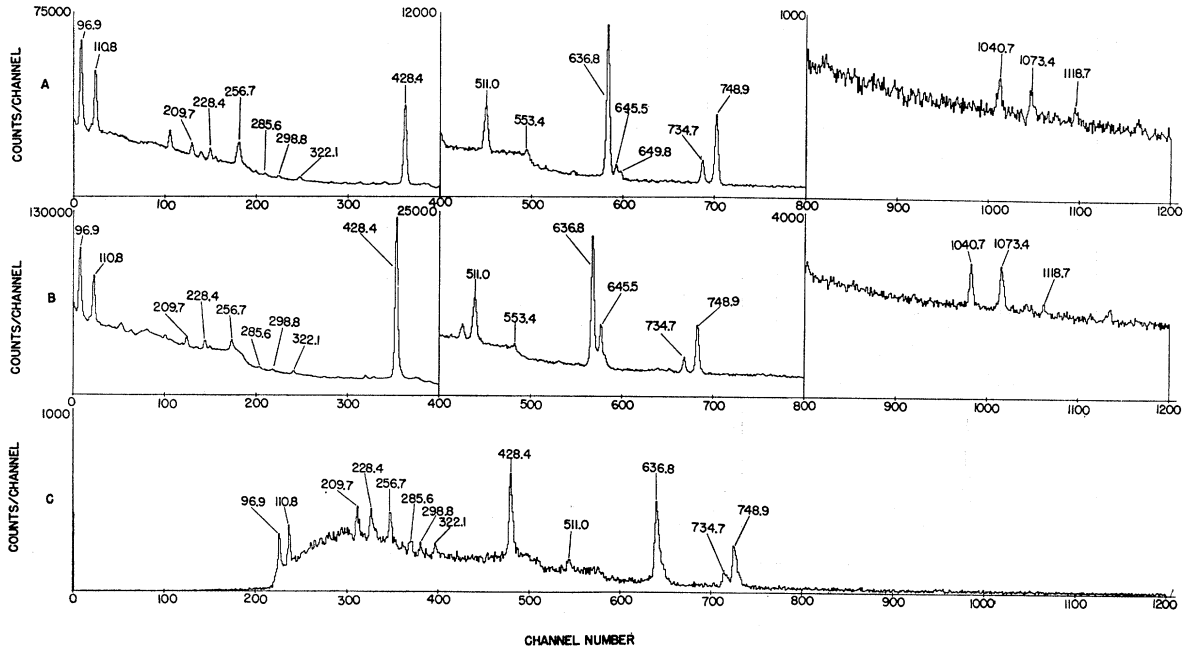

FIG. 4. γ-ray spectra from the decay of Tl^{194}: (A) from lead target, (B) from uranium target, (C) in coincidence with the 428.4-keV line.

TABLE I. Transition energies and relative γ-ray intensities for some transitions following the decay of high- and low-spin isomers of Tl^{192}, Tl^{194}, Tl^{196}, and Tl^{198}.

Mass	Transition energy[a]	Relative γ-ray intensity[b] Pb	U	Follows decay of[c]
192	133.1 ±0.5	20.6		7^+
	174.3 ±0.5	41.7	52.7	7^+
	423.0 ±0.5	329	507	2^-, 7^+
	634.7 ±0.5	238	288	2^-, 7^+
	674.2 ±1.0			2^-
	691.0 ±0.7	22.5	40.1	2^-
	745.3 ±0.6	85.5	89.6	7^+
	786.1 ±0.6	100	100	7^+
	1113.0 ±1.0	16.1	33.5	2^-
194	96.9 ±0.08[d]	10.7	9.1	7^+
	110.8 ±1.0	7.6	7.3	7^+
	209.7 ±1.0	7.1	6.7	7^+
	228.4 ±1.0	7.3	7.3	7^+
	256.7 ±1.5[e]			
	298.8 ±1.0	2.2		7^+
	322 ±2	6.5		7^+
	428.4 ±0.5	232	610	2^-, 7^+
	553.4 ±1.0			7^+
	636.8 ±0.5	151	189	2^-, 7^+
	645.5 ±0.7	14.4	65.0	2^-
	734.7 ±0.5	30.7	28.7	7^+
	748.9 ±0.5	100	100	7^+
	1040.7 ±1.0	8.4	24.4	2^-
	1073.4 ±1.0	6.5	30.5	2^-
	1118.7 ±1.0			7^+
196	84.03±0.09[d]			7^+
	222.9 ±1.0	6.1	5.4	7^+
	301.5 ±1.2	9.4	8.2	7^+
	344.9 ±1.0	2.1		
	426.3 ±0.5	222	827	2^-, 7^+
	495.8 ±1.2		5.9	2^-
	505.2 ±0.7	14.0		7^+
	588.8 ±0.7	3.7		7^+
	610.6 ±0.6	13.7	176	2^-
	635.3 ±0.5	125	264	2^-, 7^+
	695.4 ±0.5	100	100	7^+
	723.5 ±0.6	5.9	6.0	7^+
	862.1 ±1.2		6.7	2^-
	900.7 ±1.0			7^+
	964.8 ±0.7	4.9	74.5	2^-
	1024.8 ±1.0	2.3	22.2	2^-
	1036.4 ±1.0	3.6	51.4	2^-
	1105.5 ±1.5		11.4	2^-
	1190.0 ±1.2		14.8	2^-
	1388.7 ±1.2		48.0	2^-
	1434.4 ±1.2		29.1	2^-
	1496.1 ±1.2	9.5	128	2^-
	1510.6 ±1.2	3.0	19.8	2^-
	1552.8 ±1.2		78.3	2^-
196	1622.5 ±1.5		72.0	2^-
	2010.8 ±1.5		65.9	2^-
	2211.6 ±1.5		54.9	2^-
198[f]	48.32±0.11[d]			7^+
	226.8 ±0.5	4.3		7^+
	275.2 ±1.0		10	2^-
	412.0 ±0.4	176		2^-, 7^+
	480.8 ±1.2		18.2	2^-
	489.8 ±0.6	5.7		7^+
	518.9 ±1.5			7^+
	563.0 ±0.5			2^-
	587.4 ±0.7	100		7^+
	596.3 ±0.7		11.3	2^-
	606.1 ±0.8		6.9	2^-
	636.6 ±0.5	92.3		2^-, 7^+
	675.8 ±0.7	9.9	100	2^-
	744.3 ±1.2		8.7	2^-
	759.5 ±1.0		17.1	2^-
	798.7 ±1.0		12.5	2^-
	810.0 ±1.0		8.2	2^-
	876.3 ±0.8		7.4	2^-
	941.7 ±1.3			2^-
	1007.3 ±1.0		23.4	2^-
	1018.2 ±1.0		26.8	2^-
	1045.9 ±2.0			2^-
	1088.1 ±1.5		31.2	2^-
	1169.0 ±1.0		13.1	2^-
	1200.9 ±1.2	5.3	77.6	2^-
	1218.8 ±1.2			2^-
	1312.3 ±1.0		38.4	2^-
	1421.0 ±1.5		76.0	2^-
	1436.1 ±1.8		29.5	2^-
	1447.2 ±1.0		36.5	2^-
	1463.6 ±1.0		11.0	2^-
	1489.5 ±1.0		26.9	2^-
	1558.8 ±1.0			2^-
	1593.7 ±1.0		24.3	2^-
	1659.0 ±1.2		14.2	2^-
	1721.6 ±1.2		20.4	2^-
	1832.9 ±1.5		28.0	2^-
	1858.1 ±1.5		8.1	2^-
	1874.9 ±1.5		5.7	2^-
	1900.2 ±2.0		16.7	2^-
	2041.2 ±1.5		74.0	2^-
	2191.6 ±1.5		16.9	2^-
	2371.8 ±2.0		3.9	2^-
	2466.6 ±2.0			2^-
	2486.8 ±2.0		6.7	2^-
	2782.9 ±2.0			2^-

[a] Errors for transition energies are based on statistical deviations for several measurements and allowance for systematic errors in the calibration technique.

[b] Pb and U refer to sources separated from lead or uranium targets, respectively. For mass-192, -194, and -196 sources there is negligible feeding of the 2^- state by the isomeric transition and the intensities in the Pb column may be compared with those in the U column. Normalization in each case is to a transition fed only by the 7^+ isomer. A comparison of these two columns is not possible for mass 198 because of the isomeric feeding; the Pb column is derived from a measurement made shortly after separation when the admixture from the decay of the 2^- isomer was a minimum. The U column contains relative intensities only for those transitions following the 2^- isomer. Errors for intensities may be taken as: 15% for intensities greater than 50, 20% for intensities in the range 20–50, 50% for intensities in the range 5–20, and 100% for intensities less than 5.

[c] The two isomeric states are symbolized by their spins and parities.

[d] This transition energy was obtained from permanent-magnet spectrograph plates.

[e] A major part of the intensity of this transition may be due to Tl^{193} contamination. However it does appear in a coincidence spectrum and at least part must be associated with the Tl^{194} decay.

[f] Many of the transitions following the decay of Tl^{198g} have been included in a level scheme for Hg^{198} in a report by Sakai *et al.* (Ref. 19).

at 645.5, 1040.7, and 1073.4 keV relative to Fig. 4(A) is apparent. The unlabeled peaks have been associated with the decay of adjacent-mass contaminants.

In addition to coincidence experiments similar to those carried out for Tl^{192}, conversion-electron-γ coincidences were measured for Tl^{194}. The γ-γ results obtained with a 428-keV NaI gate in coincidence with a Ge(Li) detector are shown in Fig. 4(C). A comparison with a similar spectrum gated just below the 428-keV line indicates that the 428.4-keV transition is in coincidence with transitions at 96.9, 110.8, 209.7, 228.4, 256.7, 285.6, 298.8, 322.1, 636.8, 734.7, and 748.9 keV. The NaI-NaI and orange-spectrometer–NaI coincidence results can be used to establish that the 96.9-,

428.4-, 636.8-, and 748.9-keV transitions are in mutual coincidence.

A conversion-electron spectrum taken with a Si(Li) detector from a lead-separated source is shown in Fig. 5.

TABLE II. Internal conversion coefficients (C.C.) for some transitions following the decay of Tl^{192}, Tl^{194}, Tl^{196}, and Tl^{198}.

Mass	Energy	Shell	Measured C.C.[a]	Theoretical C.C.[b] $E1$	$E2$	$M1$
192	133.1	L	105	3	103	46
	174.3	K	6.7	8.7	24	140
	634.7	K	1.3	0.45	1.2	4.3
	691.0	K	1.6	0.38	0.98	3.5
	745.3	K	0.94	0.34	0.84	2.9
	786.1	K	0.30	0.30	0.76	2.5
194	96.9	L	420	6.3	431	112
	636.8	K	1.4	0.45	1.2	4.3
	645.5	K	2.9	0.44	1.1	4.2
	734.7	K	1.1	0.34	0.86	2.9
	748.9	K	0.34	0.34	0.84	2.8
196	610.6	K	2.1	0.49	1.3	4.8
	635.3	K	1.4	0.45	1.2	4.3
	695.4	K	0.41	0.38	0.98	3.5
198	587.4	K	0.48	0.54	1.4	5.3
	636.6	K	0.92	0.45	1.2	4.3
	675.8	K	1.5	0.40	1.0	3.7

[a] Values listed have been multiplied by 100. Errors range from 20% for strongest lines to 30% for weaker ones.
[b] M. E. Rose, *Internal Conversion Coefficients* (Interscience Publishers, Inc., New York, 1958). L coefficients are a sum of three subshells. The listed values have been multiplied by 100.

The labeled lines are those that have been established as following the decay of Tl^{194}. Figure 6 contains a photograph of permanent-magnet spectrograph plates that have been exposed to sources of Tl^{194}, Tl^{196}, and Tl^{198}. The conversion lines from the low-energy $E2$ transitions are clearly visible on each plate.

Tl^{196}

γ-ray spectra from the decay of Tl^{196} are given in Fig. 7. Again Fig. 7(A) is a spectrum taken with a lead-separated source and a comparison may be made with the spectrum from a uranium-separated source shown in Fig. 7(B). The enhancement of lines such as those at 610.6, 964.8, and 1036.4 keV as well as the increased complexity of the spectrum, especially above 700 keV, is evident. A number of the unlabeled low-energy peaks have been identified with the decay of Pb^{196} and some of the higher-energy lines may also result from this decay since it has not been studied above 800 keV.

A NaI-Ge(Li) coincidence spectrum is shown in Fig. 7(C). The NaI gate was set both on and below the 426.3-keV line. Comparison of these spectra indicated that the 426.3-keV transition is in coincidence with lines at 222.9, 301.5, 344.9, 426.3, 505.2, 635.3, and 695.4 keV. An unusually large contamination from adjacent Tl^{197} was observed in the singles spectrum from this source. This is particularly unfortunate here since there

TABLE III. Coincidence relationships among prominent γ rays in the decay of Tl^{192}, Tl^{194}, Tl^{196}, and Tl^{198}. The leftmost column contains energies of lines used as gates for coincidence spectra.

Mass		133.1	174.3	423.0	634.7	745.3	786.1						
192	423.0	Yes	Yes	No	Yes	Yes	Yes						
	634.7	Yes	Yes	Yes	No								
	745.3	No	Yes	Yes	Yes								
		96.9	110.8	209.7	228.4	256.7	298.8	322	428.4	636.8	645.5	734.7	748.9
194	96.9								Yes	Yes			Yes
	428.4	Yes	Yes	Yes	Yes	Yes	Yes	Yes	No	Yes	Yes	Yes	Yes
	636.8								Yes	No			Yes
	734.7								Yes	Yes		No	No
	748.9												
		229.9	301.5	344.9	426.3	505.2	610.6	635.3	695.4				
196	84.0				Yes			Yes	Yes				
	426.3	Yes	Yes	Yes	No	Yes	Yes	Yes	Yes				
	505.2				Yes			Yes	Yes				
	635.3				Yes	Yes		No	Yes				
	695.4				Yes			Yes	No				
		226.8	275.2	412.0	489.8	518.9	587.4	636.6	675.8	759.5	1200.9	1312.3	
198	48.3	Yes		Yes			Yes	Yes					
	412.0	Yes	Yes	No	Yes	Yes	Yes	Yes	Yes	Yes	Yes	Yes	

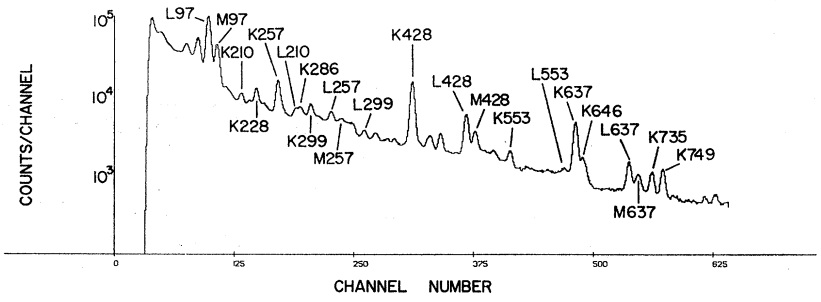

FIG. 5. Conversion-electron spectrum from the decay of Tl^{194}.

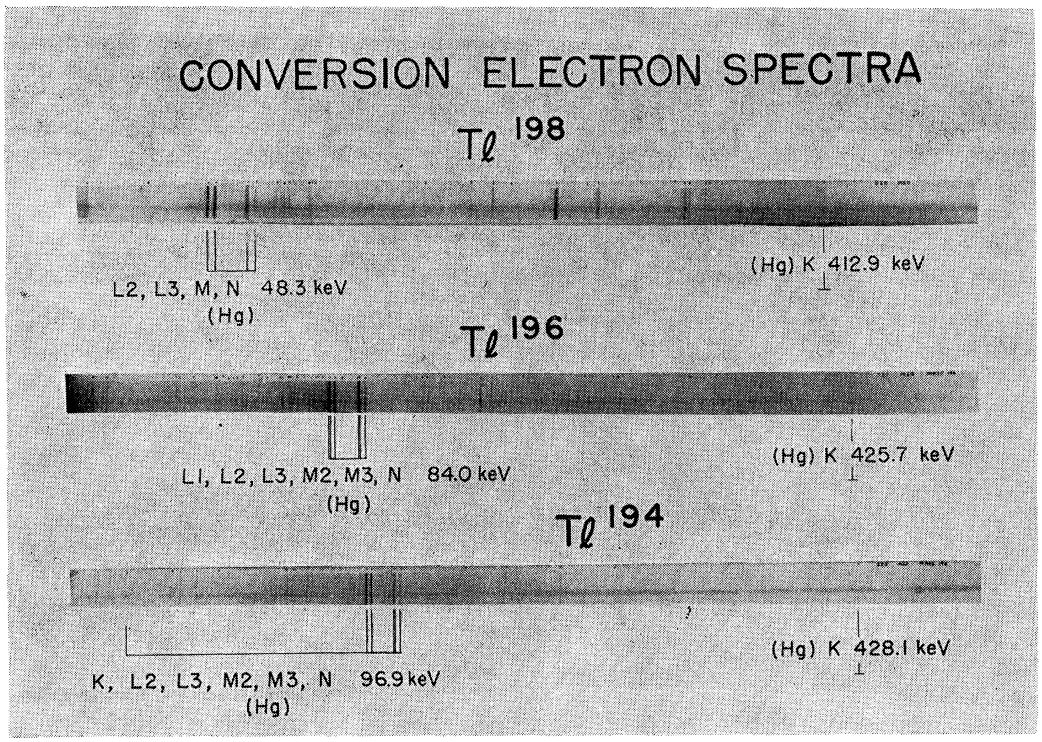

FIG. 6. Conversion-electron spectra from the decay of Tl^{194}, Tl^{196}, and Tl^{198} taken with a permanent-magnet spectrograph.

is a rather strong 426-keV transition following the decay of Tl^{197} in coincidence with a number of strong low-energy transitions, and these show up clearly as the unlabeled lines in Fig. 7(C). As for the case of Tl^{194}, the additional γ-γ and conversion-electron-γ coincidence data can be used to establish a mutual coincidence relation among the transitions at 84.0, 426.3, 635.3, and 695.4 keV. A further coincidence relation is found between the 505.2-keV line and transitions at 426.3, 635.3, and 695.4 keV by using the orange spectrometer to gate

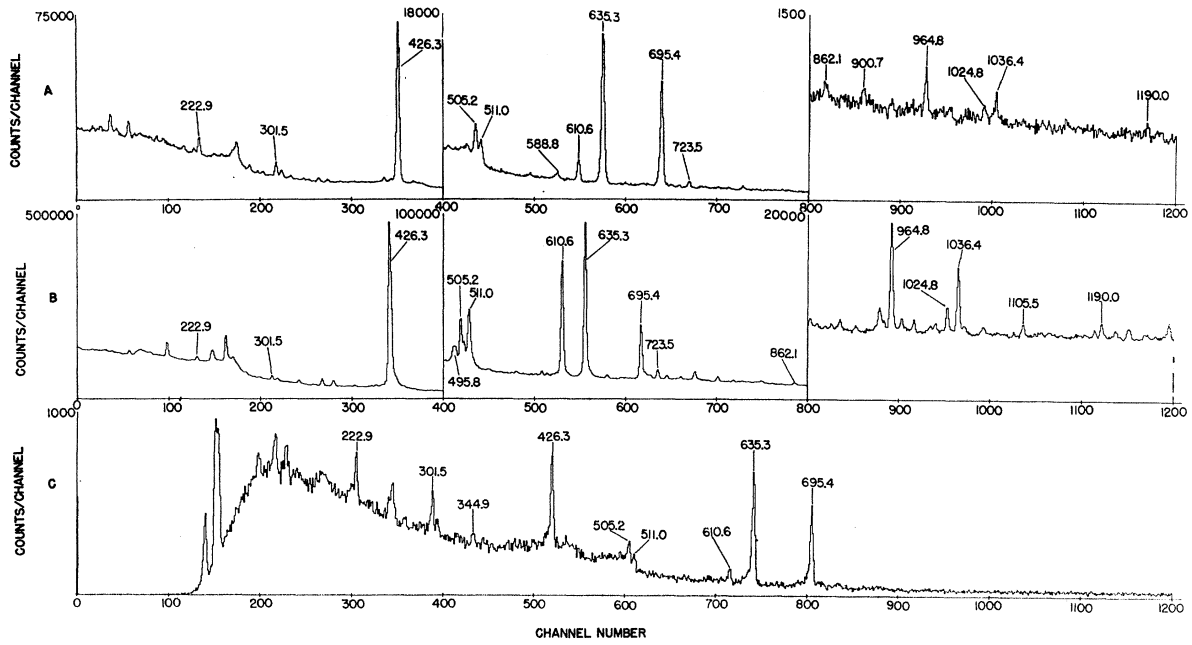

FIG. 7. γ-ray spectra from the decay of Tl^{196}: (A) from lead target, (B) from uranium target, (C) in coincidence with 426.3-keV line.

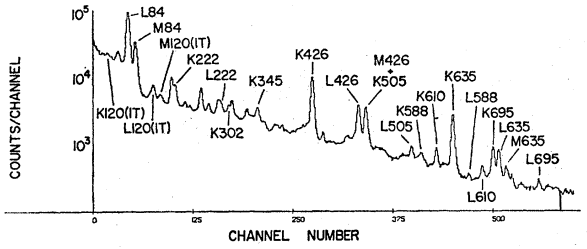

FIG. 8. Conversion-electron spectrum from the decay of Tl^{196}. IT stands for isomeric transition.

a NaI spectrum on the K-conversion line of the 505.2-keV transition.

Figure 8 contains a conversion-electron spectrum taken with a Si(Li) detector from a lead-separated source.

Tl^{198}

The fact that there is a sizable branch to the isomeric transition in the decay of Tl^{198m} makes it possible to separate transitions following the decay of the high-spin isomer from those following the ground-state decay without the necessity for uranium-separated sources. γ-ray spectra from the decay of Tl^{198} are shown in Fig. 9. The spectrum in Fig. 9(A) was taken with a lead-separated source shortly after the separation. Notice the relative simplicity of the decay of the high-spin isomer compared to that of the ground state. A spectrum taken with a uranium-separated source is compared in Fig. 9(B) and reflects, as in the case of Hg^{196}, the increased complexity of the ground-state decay. The very strong unlabeled peaks at lower energies in this spectrum have been identified with the decay of Pb^{198}.

The coincidence measurements made for this decay were analogous to those described for the mass-194 and -196 isotopes. A Ge(Li) spectrum gated on the 412.0-keV transition by a NaI detector is shown in Fig. 9(C). A comparison with a similar spectrum gated just below the 412.0-keV line indicates that the 412.0-keV transition is in coincidence with transitions at 226.8, 275.2, 489.8, 518.9, 587.4, 636.6, 675.8, 759.5, 1200.9, and 1312.3 keV. As with the other isotopes, the four strong transitions following the decay of Tl^{198m} are found to be in coincidence with each other.

A conversion-electron spectrum taken with a Si(Li) detector is given in Fig. 10. The $M4$ isomeric transition at 261 keV and the transition following it at 283.2 keV are prominent in the low-energy region.

IV. LEVEL SCHEMES

Level schemes for the four mercury isotopes studied are proposed in Fig. 11. These involve principally the transitions following the decay of the 7^+ isomer and are based on coincidence results, energy sums, intensity balances, and to some degree on energy-level systematics. Spins and parities are suggested for these levels on the basis of β-decay selection rules and measured γ-ray multipolarities, again with some resort to level systematics.

Each level scheme contains as its dominant feature a four-component cascade that is well established by a variety of coincidence experiments (see Sec. III). The first excited 2^+ states in Hg^{196} and Hg^{198} have been

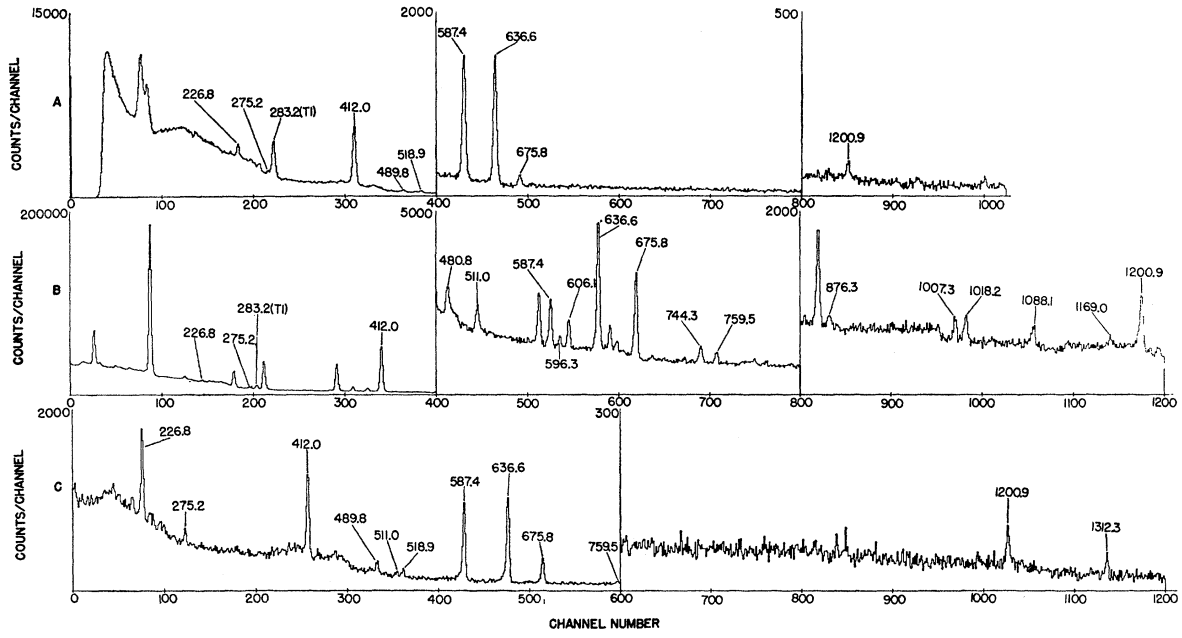

FIG. 9. γ-ray spectra from the decay of Tl^{198}: (A) from lead target, (B) from uranium target, (C) in coincidence with the 412.0-keV line.

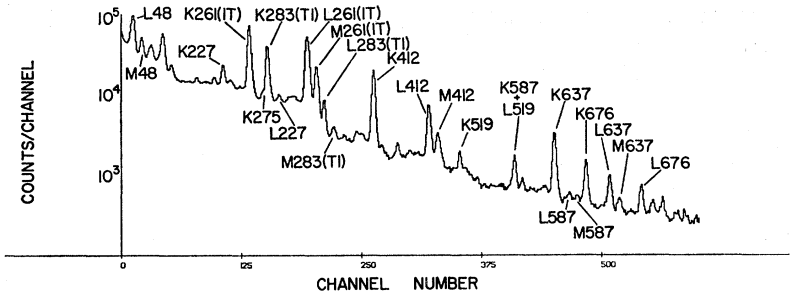

FIG. 10. Conversion-electron spectra from the decay of Tl^{198}. IT stands for isomeric transition.

thoroughly studied previously through the longer-lived decay of Au^{196} and Au^{198}.[7] Since the strongest transitions following the decay of both Tl^{192} and Tl^{194} are found to have quite similar energies and an $E2$ multipolarity, they may reasonably be assigned to the de-excitation of the first excited 2^+ level in Hg^{192} and Hg^{194}. Each of these transitions is also the strongest line in the four-member cascade. The ordering of the two higher-energy transitions for each case is made according to intensity. The low-energy transition in each cascade is placed above the other three, both for intensity reasons and for reasons described below. With these basic similarities established, each individual isotope will be considered briefly.

Hg^{194}

The four-member cascade is established by triple coincidence and conversion-electron-γ coincidence experiments. The ordering of the 428.4-, 636.8-, and 748.9-keV lines is made according to intensities as stated above. In view of the $E2$ character of the line at 636.8 keV and the absence of a crossover transition to the ground state, this level at 1065 keV is assigned a spin and parity of 4^+. The $E1$ multipolarity of the 748.9-keV transition and the absence of any crossover transitions to spin-2 states then require a spin and parity assignment of 4^- or 5^- for the level at 1814 keV. The 96.9-keV $E2$ transition is placed above these in the cascade to connect the 1814-keV level with one at 1911 keV. The 96.9-keV transition has been found to be nearly pure $E2$,[10] and since no transitions from the 1911-keV level to lower 2^+ and 4^+ states are observed, a spin and parity assignment of 6^- or 7^- is preferred.

The strong intensity of the four-member cascade can be accounted for only if the 1911-keV level is fed from the 7^+ isomer through a first-forbidden β transition. Comparison of intensities between the lead-separated and uranium-separated sources indicates feeding of the 2^+ and 4^+ levels from the ground-state decay either directly or through the population of higher-excited levels.

The second 2^+ level at 1074 is supported by the coincidence relation between the 428.4- and 645.5-keV transitions and the sum relation with the 1074-keV crossover transition. The placement of a 6^+ level at 1800 keV is based on the measured $E2$ and $E1$ multipolarities of the 734.7- and 110.8-keV transitions, respectively, and energy sum and coincidence relationships. The inclusion of this level is also supported by the work of Yamazaki and Hendrie.[9]

Hg^{196}

Arguments for placement of the first six levels exactly parallel those made for Hg^{194} except for the 6^+ level at 1785 keV. The 723.5-keV transition is a much weaker line than its counterpart in Hg^{194} and no meaningful multipolarity measurement could be made. Furthermore no $E1$ transition connecting the 1841-keV level with this one was observed. Coincidence statistics were too poor to make any statement one way or the other about a coincidence relationship with either the 426.3- or 635.3-keV lines. However, Yamazaki and Hendrie[9] indicate a level at this position that is de-excited by a 725-keV γ transition, and this also agrees with the level systematics we find from Hg^{192} and Hg^{194}. Therefore, the level is shown, but it is dashed to indicate its tentative nature if based on data in this report.

An additional level at 2346 keV is included to accommodate coincidence results with the 505.2-keV transition and the energy difference of 83.7 keV between this transition and one of energy 588.8 keV.

Hg^{198}

In addition to the first 2^+ excited state, a second 2^+ level is known from the decay of Au^{196}.[7] The other three excited levels shown in Fig. 11 accommodate the four-

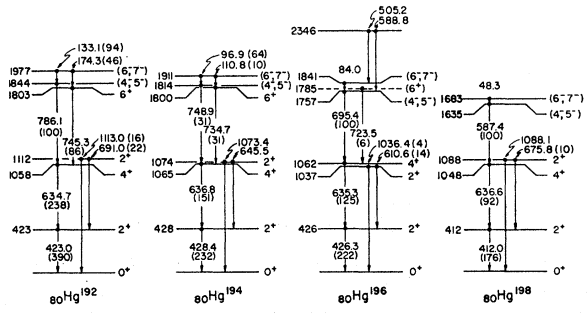

FIG. 11. Partial level schemes for Hg^{192}, Hg^{194}, Hg^{196}, and Hg^{198}. The relative γ intensities are shown in parentheses (corrected for internal conversion) and represent the total observed decays from both thallium isomeric states.

member cascade, and the spins and parities of these levels are assigned according to the discussion for Hg^{194}. No evidence for a 6^+ excited state has been found in this work. Fisher and Knapp[14] in their study of the decay of Tl^{198m} have suggested a $6^+ \rightarrow 4^+ \rightarrow 2^+ \rightarrow 0^+$ cascade in Hg^{198} based on coincidences between a sequence of 637-, 588-, and 411-keV γ rays. Our level scheme differs both in the sequence of these cascading transitions and in the assignment of $E1$ multipolarity to the 588-keV γ ray.

Hg^{192}

The coincidence experiments for this isotope do not unambiguously establish the four-component cascade. However, there are no inconsistencies with the ordering shown, and the systematic behavior of the other three isotopes strongly supports this assignment. On this basis levels are placed at 423, 1058, 1844, and 1977 keV. The second 2^+ level at 1113 keV is based on the coincidence relationship between the 423.0- and 691.0-keV lines and the corresponding sum relationship of these with the observed 1113.0-keV crossover transition. The placement of a 6^+ level at 1803 keV follows directly the same arguments used for the corresponding level in Hg^{194}.

V. DISCUSSION

A comparison of the low-lying positive-parity states now known for the even isotopes of mercury is given in Fig. 12. The spacing of these levels is remarkably independent of the neutron number of each isotope, especially for the four studied in this paper. To further illustrate the similarities, the ratios of the energies of certain excited states to the energy of the first 2^+ state are given in Table IV. For the isotopes $Hg^{192,194,196,198}$ the similarity of the corresponding ratios is apparent; the maximum variation for ratios involving the first 4^+ and 6^+ states is less than 2%. These ratios of approximately 2.5 and 4.25 lie midway between the ratios predicted for a vibrating spherical nucleus on the one hand and a rigid rotating spheroidal nucleus on the other. These energy ratios may also be compared to those known for some neighboring nuclei by making use of a plot originated by Nathan and Nilsson.[15] Such a plot is shown in Fig. 13 for Hg^{194}, Pt^{190}, Os^{190}, and Os^{182}, where Hg^{194} is chosen as representative of the even mercury isotopes. Again the mercury ratios lie about midway between rotational and vibrational limits, though of the four examples included Hg^{194} most closely approaches the vibrational limit. It would be of interest to locate states with even higher spins in the even mercury isotopes in order to follow the spacing trends. It is worthwhile to point out that, while the energy spectra of the mercury isotopes are so similar as discussed above, significant variation in the detailed structure of these isotopes is expected. For example, the effective quadrupole deformation parameter β_2/β_{2sp} (in single-particle units) may be determined for the previously studied stable, even mercury isotopes from the tabulated reduced transition probabilities for the $E2$ transitions depopulating the first excited 2^+ states.[16] This deformation decreases rapidly with increasing neutron number, from a value of 6.4 for Hg^{196} to 2.4 for Hg^{204}. This may be compared, for example, with the value 14.6 for the strongly deformed nucleus Er^{166}. For Hg^{192} and Hg^{194} it is likely therefore that the $E2$ enhancement factors are in excess of 25% of those known for the strongly deformed rare-earth nuclei.

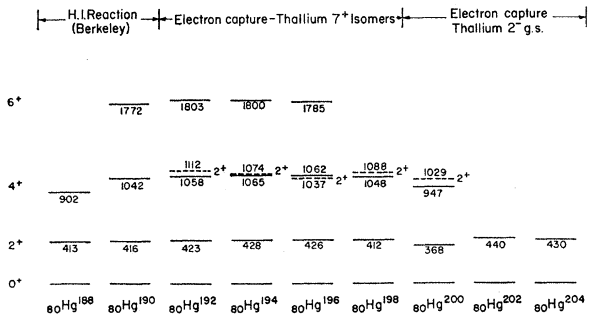

FIG. 12. Comparative level schemes for mass-188 through mass-204 isotopes of mercury. The data for Hg^{188} and Hg^{190} are from Diamond *et al.* [Nucl. Phys. **A92**, 306 (1967)] and the data for Hg^{200}, Hg^{202}, and Hg^{204} are from Lederer *et al.* (Ref. 7).

TABLE IV. Ratios of level energies to the energy of the first excited 2^+ state in some even-mass mercury isotopes.

Ratio \ Mass	188[a]	190[a]	192	194	196	198	200[b]
$R_{2^{+\prime}}$			2.63	2.51	2.43	2.64	2.80
R_{4^+}	2.18	2.50	2.50	2.49	2.49	2.54	2.57
R_{6^+}		4.26	4.26	4.20	4.19		
$R_{(4,5)^-}$			4.36	4.24	4.12	3.97	

[a] Data from Burde *et al.* [R. M. Diamond and F. S. Stephens, Nucl. Phys. **A92**, 306 (1967)].
[b] Data from Sakai *et al.* (Ref. 19).

The radiative $E2$ to $M1$ branching ratios ($\delta^2 = E2/M1$) may be calculated for the transition between the second 2^+ excited state ($2^{+\prime}$) and the first 2^+ excited state in $Hg^{192,194,196}$ using the experimental and theoretical conversion-coefficient data from Table II. The results of this calculation are presented in Table V along with the results of Sakai, Nozawa, Ikagami, and Yamazaki[17] and of Koch, Münnich, and Schötzig[18] for comparison in the case of Hg^{198}. Clearly there is considerable $M1$ admixture in these $2^{+\prime} \rightarrow 2^+$ transitions, and this admixture

[14] P. S. Fisher and V. Knapp, Proc. Phys. Soc. (London) **A69**, 541 (1956).

[15] *Alpha-, Beta-, and Gamma-Ray Spectroscopy*, edited by K. Siegbahn (North-Holland Publishing Co., Amsterdam, 1965), 2nd ed., Vol. I, Chap. 10.

[16] P. H. Stelson and L. Grodzins, Nucl. Data **1**, 21 (1965).

[17] M. Sakai, M. Nozawa, H. Ikegami, and T. Yamazaki, Nucl. Phys. **53**, 529 (1964).

[18] J. Koch, F. Münnich, and V. Schötzig, Nucl. Phys. **A103**, 300 (1967).

cannot be explained on the basis of simple phenomenological models involving rotations and vibrations.

The ratios of the $B(E2)$ strengths for the crossover to cascade transitions depopulating the $2^{+\prime}$ level may be computed for $Hg^{192,194,196,198}$ using the observed relative γ intensities for these transitions. The results are shown in Table V, where corrections have been made for the $M1$ admixture in the $2^{+\prime} \rightarrow 2^+$ transition.

The character of the transitions between the two negative-parity states proposed for each isotope is probably best revealed by the measured conversion coefficients for the low-energy transitions connecting these two levels. Using the measured and theoretical L conversion coefficients from Table II for Hg^{192} and Hg^{194}, one may ascertain that these transitions contain less than 5% $M1$ admixture. Jung and Andersson[10] also found the analogous transitions in Hg^{196} and Hg^{198} to be quite pure $E2$, and on this basis a spin difference of 2 between these two negative-parity levels is strongly suggested.

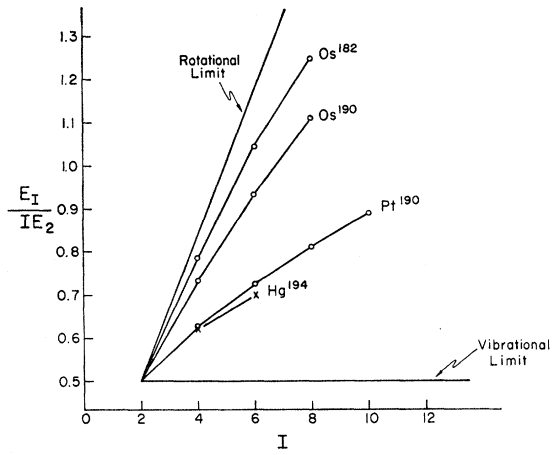

FIG. 13. $[E_I/IE_2]$ versus I for Os^{182}, Os^{190}, Pt^{190}, and Hg^{194}.

For Hg^{192} and Hg^{194} it is possible to compare the energy-reduced radiative transition probabilities for the competing $E2$ and $E1$ transitions from the higher-energy negative-parity level from the relative γ intensities from Table I. Values of 60 and 200 MeV^{-2} are obtained for the ratio $\|\Gamma_{E2}\|/\|\Gamma_{E1}\|$ for Hg^{192} and Hg^{194}, respectively, and are constant to within a factor of 4. These values may be compared with the ratio obtained from the Weisskopf estimate which is 2.4×10^{-5} MeV^{-2}. The deviation most likely indicates a hindrance of the $E1$ transition by a factor greater than 2×10^6, assuming the $E2$ transition is not enhanced.

Sufficient information is available to compute the logft value for the electron-capture transition from the 7^+ isomeric level in Tl^{198} to the upper negative-parity level in Hg^{198}. Sakai *et al.*[19] find a decay energy of 3350 keV for the decay of the ground state of Tl^{198} to the ground state of Hg^{198} while Jung and Andersson[10] locate the 7^+ isomeric state of thallium 544 keV above the ground state. Using 1684 keV for the energy of the upper negative-parity level we obtain a decay energy of 2210 keV for the electron-capture decay from the 7^+ state in Tl^{198} to an upper negative-parity state in Hg^{198}. The ratio of the intensity of the 48.3-keV transition in Hg^{198} to the intensity of the 7^+ to 2^- isomeric transition in Tl^{198} has been reported to be 1.2 ± 0.1.[10] Our data indicate that the 48.3-keV transition occurs in 57% of the total electron-capture transitions of the 7^+ isomeric state. Using these data, the measured half-life of 1.87 h, and allowing for a 20% positron branch, we obtain a logft for this decay of 6.3.

TABLE V. $E2$-$M1$ mixing ratios ($\delta^2 = E2/M1$) and $B(E2)$ ratios for the $2^{+\prime} \rightarrow 2^+ \rightarrow 0^+$ cascades in $Hg^{192,194,196,198}$.

	Hg^{192}	Hg^{194}	Hg^{196}	Hg^{198}
δ^2	$3.2_{-1.4}{}^{+4.1}$	$0.7_{-0.7}{}^{+8.6}$[a]	$3.4_{-1.5}{}^{+4.4}$	1.8 ± 0.24[b] $2.0_{-0.33}{}^{+0.48}$[c]
$\frac{B(E2;2^{+\prime}\rightarrow0^+)}{B(E2;2^{+\prime}\rightarrow2^+)}$[d]	1.0×10^{-1}	2.9×10^{-2}	2.8×10^{-2}	4.3×10^{-2}

[a] The large uncertainty in this case is due to the difficulty in estimating the contribution of the 649.8-keV line to the conversion-electron intensity of the 645.5-keV line for the determination of the conversion coefficient [see Figs. 4(A) and 5].
[b] From Koch *et al.* (see Ref. 18).
[c] From Sakai *et al.* (see Ref. 19).
[d] In correcting the γ-ray intensities for $M1$ admixture, a weighted average of $\delta^2 = 3.0$ was used for $Hg^{192,194,196}$. Errors for the values given are roughly 50% for $Hg^{192,196,198}$ and 100% for Hg^{194}.

The simplest phenomenological model capable of an approximate description of the relative ordering of the low-lying even-parity states in the even-even mercury isotopes is probably the rigid asymmetric-rotor model of Davydov and Fillipov.[20] In order to set the asymmetry parameter γ of this model, one can note the close proximity of the $2^{+\prime}$ and 4^+ states, which indicates a γ of approximately 22° [20] and the observed energy ratio $E_{2^{+\prime}}/E_{2^+} = 2.5$, which is indicative of a γ of approximately 24°.[21] If values of γ from 22° to 30° (the maximum possible asymmetry) are taken, the model predicts values of 5.0–5.5 for the energy ratio E_{6^+}/E_{2^+}, which is considerably higher than the ratio 4.2 found in this work. Such a discrepancy could possibly be accounted for by considering rotation-vibration coupling. It is interesting to note that the ratio $B(E2;2^{+\prime}\rightarrow0^+)/B(E2;2^{+\prime}\rightarrow2^+)$ predicted by this model for $\gamma = 22°$ and $\gamma = 24°$ is 1.2×10^{-1} and 6.6×10^{-2}, respectively, which are consistent with the experimental values in Table V.

One obvious difficulty with the asymmetric-rotor model is that it predicts a 3^+ state located above the $2^{+\prime}$ state by an energy interval equal to the energy of the first excited 2^+ state. Though such levels have been found in the even-even isotopes of platinum and

[19] M. Sakai, H. Ikegami, T. Yamazaki, and M. Nozawa, in *Congrès International de Physique Nucleaire* (Editions du Centre National de la Recherche Scientifique, Paris, 1964), p. 505.

[20] A. S. Davydov and G. F. Fillipov, Nucl. Phys. 8, 237 (1958).
[21] G. R. DeMille, T. M. Kavanagh, R. B. Moore, R. S. Weaver, and W. White, Can. J. Phys. 37, 1036 (1959).

osmium[7] they seem to be absent for the even-even mercury isotopes.

Semimicroscopic calculations of the states in some even-mass mercury isotopes have recently been reported by both Alaga and Ialongo[22] and Covello and Sartoris.[23] In these calculations the two proton holes are coupled to a vibrational core with a residual interaction between the holes. Energies and transition probabilities for transitions between excited states of Hg^{198} have been tabulated by Covello and Sartoris,[23] and these may be compared with experimental values. According to the calculation of these latter authors, $B(E2; 2^{+\prime} \rightarrow 0^+)/B(E2; 2^{+\prime} \rightarrow 2^+)$ is 0.14, approximately seven times larger than the experimental value. They calculate a value of $\delta^2 = 1.17$ for the $E2$ to $M1$ mixing ratio for the $2^{+\prime} \rightarrow 2^+$ transition in comparison to the measured value of 2.0. This model also predicts the existence of negative-parity levels based on the inclusion of an $h_{11/2}$ single-particle hole state which leads to negative-parity levels of spins 5, 6, or 7. However, these levels occur much higher in the theoretical spectrum than those observed experimentally, and the authors conclude that such a model is too crude to provide an adequate description of the negative-parity states.[24]

Finally, some comment should be made concerning the apparent absence of significant electron capture from the 7^+ isomer in the thallium isotopes to the 6^+ state in the mercury daughters. By considering the relative intensities associated with the γ transitions in Fig. 11 one can conclude that less than 15% of the electron-capture events proceed via this decay, although it is formally allowed under Gamow-Teller selection rules. A simple qualitative explanation of this observation may be made on the basis of the shell model. A coupling of the odd $s_{1/2}$ proton and $i_{13/2}$ neutron in thallium can give a positive parity level of spin 7. The electron-capture decay of thallium to a 6^+ level in mercury in which the next available neutron state was filled would therefore require the transition of an $s_{1/2}$ proton into an $i_{13/2}$ neutron, a transition that would be highly forbidden. On the other hand, the first-forbidden transitions of an $s_{1/2}$ proton to a $p_{1/2}$ neutron or an $h_{11/2}$ proton to an $i_{13/2}$ neutron give rise to an open neutron or proton configuration which can be coupled to give states of negative parity and spins 6 or 7. The $E1$ transitions from such states to the lower-lying positive-parity levels would be expected to be highly hindered so that measurement of these lifetimes would be of interest.

It may be noted that Alaga[25] has recently discussed this β-decay hindrance from the point of view of the intermediate-coupling model involving two proton holes. He points out that according to his calculation the lowest even-parity states in Hg^{198} have similar quadrupole moments and, therefore, presumably similar intrinsic structure. He suggests that the hindrance of the electron-capture decay to the 6^+ level in mercury reflects the special similarity between this level and the 0^+ ground state which would then be members of a collective sequence. The hindrance is analogous to the K-forbidden transitions found in the highly deformed nuclei.

Both of the explanations mentioned above for the hindrance of the $7^+ \rightarrow 6^+$ electron-capture decay suggest that the 6^+ level is a collective level based on the ground state.

ACKNOWLEDGMENTS

We are indebted to Professor M. G. White, Director of the Princeton-Pennsylvania Accelerator, and the accelerator staff for the bombardments. Appreciation is due to Georg Sidenius for his excellent guidance during the initial phases of the isotope separations and to Fred Loeser for his operation of the isotope separator. We also acknowledge many discussions with Dr. A. Covello and correspondence with Dr. G. Ialongo. We would like to thank Dr. T. Yamazaki for communicating his results on levels in Hg^{194} to us before publication. One of us (R.A.N.) would like to acknowledge helpful conversations with Professor Ben R. Mottelson and Dr. Bengt Sørensen of the Niels Bohr Institute.

[22] G. Alaga and G. Ialongo, Phys. Letters **22**, 619 (1966).
[23] A. Covello and G. Sartoris, Nucl. Phys. **A104**, 189 (1967).
[24] A. Covello and G. Sartoris (private communication).
[25] G. Alaga, notes from Enrico Fermi Summer School, Varenna, 1967 (unpublished).

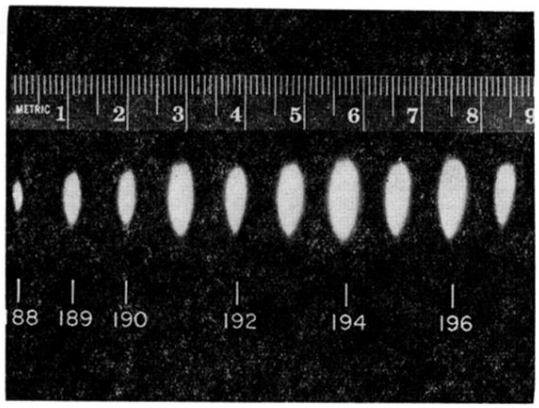

FIG. 1. Radio-autograph of the collector foil after a separation of isotopes from an irradiated lead target.

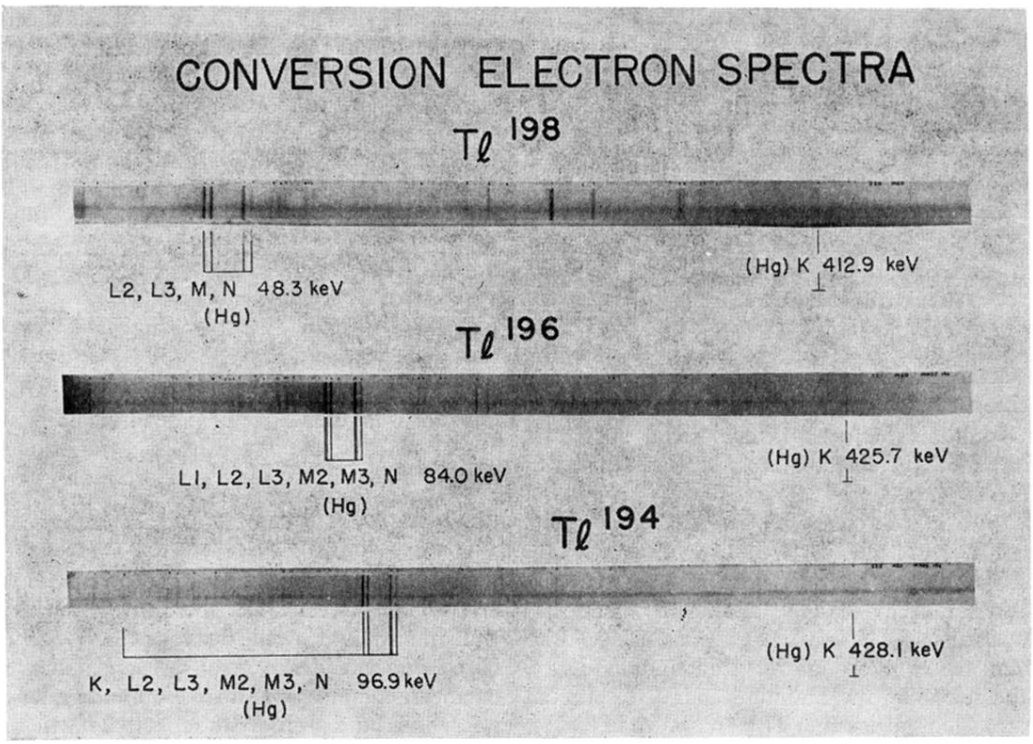

FIG. 6. Conversion-electron spectra from the decay of Tl^{194}, Tl^{196}, and Tl^{198} taken with a permanent-magnet spectrograph.